Spectrochimica Acta Part B: Atomic Spectroscopy 195 (2022) 106505

Contents lists available at ScienceDirect

Spectrochimica Acta Part B: Atomic Spectroscopy

journal homepage: www.elsevier.com/locate/sab

spICP-MS characterisation of released silver nanoparticles from (nano) textile products

Iria Rujido-Santos [a], M. Estela del Castillo Busto [b], Isabel Abad-Alvaro [b], Paloma Herbello-Hermelo [a], Pilar Bermejo-Barrera [a], María Carmen Barciela-Alonso [a], Heidi Goneaga-Infante [b], Antonio Moreda-Piñeiro [a,*]

[a] Group of Trace Element, Spectroscopy, and Speciation (GETEE), Institute of Materials iMATUS, Department of Analytical Chemistry, Nutrition, and Bromatology, Faculty of Chemistry, Universidade de Santiago de Compostela, Avenida das Ciencias, s/n 15782, Santiago de Compostela, Spain
[b] LGC Ltd, National Measurement Laboratory, Queens Road, Teddington TW11 0LY, United Kingdom

ARTICLE INFO

Keywords:
Silver nanoparticles
Textile
Mechanical stirring
Single particle inductively coupled plasma mass spectrometry

ABSTRACT

The low limits of detection and information regarding the concentration and size distribution of nanoparticles provided by single particle inductively coupled plasma mass spectrometry (spICP-MS) has been taken in advance for assessing released silver nanoparticles from (nano)textiles (nanosilver textiles). The releasing procedure consisted of using orbital-horizontal shaking (100 rpm, 20 °C, 30 min) and ultrapure water (10 mL) as an extractant, and it was found to guarantee silver nanoparticles stability (silver nanoparticle concentration and size distribution). Stability of released silver nanoparticles was further investigated at several filtration (0.22, 0.45 and 5.0 μm) and centrifugation conditions, stages required for fluff removal after extraction and just before spICP-MS determinations. Filtration using 5.0 μm filters was found to not affect silver nanoparticles concentrations and size distributions. The extractive procedure plus spICP-MS has shown a limit of detection and a limit of quantification for silver nanoparticle number concentration of 4.59×10^4 and 1.53×10^5 silver nanoparticles per gram of textile, respectively, whereas a limit of detection in size of 12 nm was obtained. Repeatability of the overall procedure was 14% (silver nanoparticle concentration) and 6% (mean silver nanoparticle size). Similarly, analytical recovery assays using standard silver nanoparticles of 20, 40, and 60 nm led to recoveries within the 102–113% range. The high degree of fixation of the AgNPs to the fabric and the softness of the extraction process to guarantee the integrity of the nanoparticles has led to a non-quantitative extraction (extraction percentages between 0.3 and 9.0% depending on the textile sample). However, the methodology developed has proven to be highly efficient for the characterization of the extracted AgNPs, and robust since the stability of the released AgNPs during the extraction procedure.

1. Introduction

Silver species such as metallic silver, silver sulfadiazine, and silver nitrate have been used since centuries to treat bacterial infections, wounds, and burns [1]. Similarly, silver nanoparticles (AgNPs) also exhibit antibacterial activity, and they are widely used as an alternative to antibiotics [2]. AgNPs also have antifungal [3] and antiviral [4] properties, which make them useful in several industrial sectors such as medicine or agriculture.

AgNPs are promising compounds used in the medical industry for manufacturing wound dressings for ulcers and burns, bone cement, catheters, hand gels, and surgical drains [5] due to their antibacterial properties. Furthermore, AgNPs are also useful in anticancer treatments [6] and as contrast agents [7]. In addition, AgNPs are used in water filtration [8], food packaging [9], cosmetics [10], appliances [11], paints [12], and textiles [13] because of their bacterial inhibition. On the other hand, AgNPs also offer excellent properties for catalysis [14] and can be useful in the fabrication of electronic devices [15].

Regarding the textile industry, fibres are modified with AgNPs mainly to obtain fabrics with antibacterial properties [16,17]. Humidity, appropriate temperature, sweat, dead skin cells, and finishing agents of textiles enhance bacterial growth on the textile surface [18]. Bacteria can discolour fibres, generate bad odour, and even deteriorate textiles [19]. The growth of bacteria in textiles can also be a risk to human

* Corresponding author.
E-mail address: antonio.moreda@usc.es (A. Moreda-Piñeiro).

https://doi.org/10.1016/j.sab.2022.106505
Received 7 June 2022; Received in revised form 13 July 2022; Accepted 21 July 2022
Available online 25 July 2022

health due to their possible propagation between textile products and human skin. This risk is minimised by textile modification with AgNPs. Furthermore, AgNPs can be used to dye fibres such as wool [20], cotton [21], silk [22], and viscose [23] based on AgNPs localised surface plasmon resonance (LSPR). The colour of fabrics is dependent on the shape and size of AgNPs. Thus, AgNPs can replace synthetic azo dyes (carcinogenic agents) which are the most used dyes in the textile industry [24].

Several immobilisation procedures by chemical modification of textiles with AgNPs have been described, mainly grouped as *ex situ* and *in situ* treatments. *Ex situ* treatments imply the textile to be soaked in an AgNPs suspension. However, *in situ* approaches are two-step methodologies: first, ionic silver is integrated in the textile yarns and subsequently, a reduction of the ionic silver to AgNPs is *in situ* carried out by using a reducing agent. In both cases, stabilising agents are used to prevent AgNPs aggregation [25].

The main drawback of textile modification with AgNPs is the lack of stability of the nanoparticles in the fibres, so AgNPs are released during fabric washing. Certain organic polymers, used as linkers between AgNPs and the fibre surface, have been proposed to enhance AgNPs durability in textile products [19].

AgNPs could be a serious risk to humans due to the possible penetration of these particles through the skin. Kraelinga et al. [26] performed *in vitro* experiments to test the penetration of coated AgNPs into human skin. These authors have concluded that less than 10% of the silver dose can be absorbed by the skin, and this small amount was located mostly in the *stratum corneum* of the epidermis, which is responsible for the protective function of the skin. However, detectable concentrations were also found in the deepest layers of skin (dermis). In addition, some *in vitro* findings suggest that AgNPs permeation with damaged skin is higher than with intact (healthy) skin [27].

Research regarding the presence AgNPs on textiles is therefore needed. The available analytical methodology is scarce and the literature deals with experiments that simulate the AgNPs lixiviation from textiles during home laundering [28–33]. Electron microscopy coupled to energy-dispersive X-ray spectroscopy (EDX) was used in several published studies for analysing the washing solutions of fabrics (AgNPs determination/characterisation) [28,29,33]. On the other hand, total silver released from textile products was assessed by inductively coupled plasma mass spectrometry (ICP-MS) or inductively coupled plasma optical emission spectrometry (ICP-OES) after acid digestion of washing solutions or washed textiles [28–33]. Furthermore, X-ray absorption near edge structure spectroscopy (XANES) was used for the direct analysis of textile solid samples (unwashed and/or washed) [30,33]. Recently, ICP-MS operating in the so-called 'single particle' mode (spICP-MS) has also been used by Mitrano et al. [33] for AgNPs assessment in simulated laundry washing wastes. Fundamentals of spICP-MS can be found elsewhere [34,35] and the main advantage of the technique consists in simultaneously supplying nanoparticle number concentration, size, and number size distribution, as well as distinguishing dissolved and particulate analytes by measuring the discrete particles (pulses) over a continuous background (dissolved species). Several applications of spICP-MS for assessing inorganic nanoparticles in biological and environmental materials can be found in the literature [36–38]. In addition, improvements focused on the use of collision/reaction gases [39,40], more robust sample introduction systems such as linear pass spray chambers to enhance nanoparticles transport efficiency (TE) [41,42], and new calibration methodologies for overcoming matrix effects [43,44] have been recently published. Similarly, great advances have been also reported for hyphenating spICP-MS with separation techniques such as scanning mobility particle sizer (SMPS) [45] and dynamic secondary ion mass spectrometry (dynamic SIMS) [46].

The aim of the current work has been the development of reliable analytical procedures for the assessment of AgNPs released from fabrics (extraction and characterisation). Sample pre-treatment strategies based on mechanical lixiviation have been investigated for AgNPs isolation from textiles, whereas, spICP-MS has been used for providing information about AgNPs concentration and size distribution.

Table 1
Brief description of analysed textiles.

Sample	Subsamples	Type	Composition
T1	T1–1 T1–2	Cycling sportswear	82% polyester, 18% elastane (product containing silver)
T2	-[a]	Socks	80% cotton, 13% polyamide, 5% silver, 2% elastane
T3	-[a]	Socks	66% polyamide, 24% elastane, 10% polyamide with silver
T4	-[a]	Men's T-shirt	100% polyester with silver
T5	-[a]	Men's T-shirt	52% Coolmax® (polyester), 44% Nanosilver® (polyester), 4% Lycra® (elastane)
T6	T6–1 T6–2	Socks	55% cotton, 30% Nanosilver® (polyester), 15% Lycra® (elastane)
T7	-[a]	Men's underwear	60% cotton, 32% Nanosilver® (polyester), 8% Lycra® (elastane)

[a] Only one subsample.

2. Materials and methods

2.1. Instrumentation

A NexION® 300× ICP-MS (Perkin Elmer, Waltham, MA, USA) with a nebulisation system composed of a Meinhard® nebuliser and a cyclonic spray chamber thermostated by a Peltier refrigerator was used to analyse digested fabrics (total Ag content) and determine/characterise AgNPs in the aqueous extracts. A SeaFast SC2 DX autosampler (Elemental Scientific, Omaha, NB, USA) was used as sample introduction system for both ICP-MS (total Ag determination) and spICP-MS (AgNPs determination and characterization). A Syngistix™ Nano Application software version 1.1 was used to perform AgNPs determination (concentration and size distribution). A HRTEM Zeiss Libra 200FE (Oberkochen, Germany) coupled to EDX spectroscopy was used for the characterisation of AgNPs in aqueous extracts from fabrics for comparative purposes. An analytical balance ML 204 T (Mettler Toledo, Colombus, OH, USA) was used for weighing reagents and samples. A Boxcult temperature-controlled incubation chamber (Stuart Scientific, Surrey, UK) equipped with a Rotabit orbital-rocking platform shaker (J. P. Selecta, Barcelona, Spain) was used to carry out the mechanical extraction of AgNPs. A VibraCell VCx 130 ultrasound probe from Sonics (Newtown, CT, USA) was used to assist AgNPs extraction from textiles. A Laborcentrifugen 2 K15 centrifuge (Sigma, Osterode, Germany) was used for the removal of fluff in textile aqueous extracts. A Raypa UCI-150 Ultrasonic Cleaner (R. Espinar S.L, Barcelona, Spain) with programmable temperature and time was used to sonicate the extracts and avoid AgNPs agglomeration. An ETHOS PLUS microwave lab-station (Milestone, Sorisole, Italy) with 100 mL closed Teflon vessels and Teflon covers was used to perform acid digestion of textile samples.

2.2. Reagents

Ultrapure water (18 MΩcm resistivity) was obtained from a Milli-Q® water purification system (Millipore, Bedford, MA, USA). 37% hydrochloric acid, 69% Hiperpur nitric acid, 33% hydrogen peroxide, and ethanol were from Panreac (Barcelona, Spain). 48% hydrofluoric acid was supplied by BDH (Poole, United Kingdom). Glycerol (99.5%), D-lactose monohydrate (99.5%), and 1-butyl-3-methylimidazolium bromide (BMIMBr) > 97% were purchased from Sigma Aldrich (San Louis, MO, USA). NexIon Setup Solution (10 μg L^{-1} of U, Pb, Mg, Li, In, Fe, Ce, and Be in 1% HNO_3) was from Perkin Elmer. Silver (1000 mg L^{-1} in 0.5 M HNO_3) and rhodium (1000 mg L^{-1} in 5% HNO_3) stock standard solutions were supplied by Merck (Darmstadt, Germany). 0.02 g L^{-1}AgNPs standards (aqueous suspensions with sodium citrate as a stabiliser) of 60

Table 2
Microwave temperature program for acid digestion of textiles.

Time (min)	Temperature (°C)
0–2	Room temperature - 150
2–7	150
7–9	150–170
9–19	170
19–20	170–200
20–40	200

Table 3
ICP-MS and spICP-MS instrumental parameters for total silver and AgNPs determination.

ICP-MS operating conditions for total Ag assessment	
Plasma gas flow (L min^{-1})	16
Auxiliary gas flow (L min^{-1})	1.2
Nebulisation gas flow (L min^{-1})	0.9–1.1
Radiofrequency power (W)	1600
Collision gas (He) cell (mL min^{-1})	1.0
Analyte	Ag (*m/z* 106.905)
Internal standard	Rh (*m/z* 102.906)

spICP-MS operating conditions and SYNGISTIX™ NANO application parameters for AgNPs assessment	
Plasma gas flow (L min^{-1})	16
Auxiliary gas flow (L min^{-1})	1.2
Nebulisation gas flow (L min^{-1})	0.85–0.90
Radiofrequency power (W)	1600
Sample flow rate (mL min^{-1})	0.40–0.45
Analyte	Ag (*m/z* 106.905)
Mode	Standard
Density (g cm^{-3})	10.49
Mass fraction (%)	100
Ionisation efficiency (%)	100
Dwell time (μs)	100
Sampling time (s)	100
Number of scanning	1
Number of readings	1,000,000

nm, 40 nm, and 20 nm were purchased from Sigma-Aldrich and Nano-Composix (San Diego, CA, USA). The reference material RM 8013 of gold nanoparticles (aqueous suspension with citrate as a stabiliser) of 60 nm nominal diameter was supplied by National Institute of Standards and Technology (Gaithersburg, MD, USA). Other consumables were cellulose acetate 0.22 μm and 0.45 μm syringe filters (Labbox Labware S. L., Barcelona, Spain), Minisart® NML surfactant-free cellulose acetate 5.0 μm syringe filters (Sartorius, Goettingen, Germany), and 10 mL sterile disposable syringes (Dispomed, Gelnhausen, Germany).

2.3. Textile samples

Samples analysed in the current study consisted of T-shirts (two samples), socks (three samples), underwear (one sample), and sportswear (one sample), as shown in Table 1. Textiles coded as T1 (men's cycling culotte) and T3 (socks) were bought in local stores in Santiago de Compostela (Spain); whereas the remaining textiles were purchased from an online market. According to the manufacturer's specifications, studied textiles contain silver (Table 1). A visual examination of textiles showed that two of them (T1 and T6) were made of fibres with different appearances. In these cases, fabrics were divided into several subsamples (Table 1). Each textile subsample was cut into small pieces (5 × 5 mm) with ceramic scissors, and textile pieces were kept in plastic bags at room temperature and protected from light.

2.4. Microwave-assisted acid digestion of textile samples

Clothing pieces (0.2000 g) were placed into PTFE digestion vessels, and 8.0 mL of 69% nitric acid, 0.5 mL of 37% hydrochloric acid, 0.5 mL of 33% hydrogen peroxide, and 1.0 mL of 48% hydrofluoric acid were added. Each vessel was closed and subjected to microwave irradiation (using the microwave temperature program shown in Table 2). The digestion procedure was performed in triplicate for each sample (or subsamples according to Table 1), and at least one blank was prepared in each digestion set. Finally, acid digests were diluted to 25 mL with ultrapure water and kept in polyethylene sealed bottles at room temperature.

2.5. Total Ag determination by ICP-MS

Acid digests from textiles were diluted with ultrapure water before their ICP-MS analysis. The adjustment of the ICP-MS parameters (nebulisation gas flow, torch position, optical lens, and quadrupole voltages) was performed daily. The *m/z* ratio monitored was ^{107}Ag, and ^{103}Rh (10 μg L^{-1}) was used as an internal standard. Standard addition calibrations (0–100 μg L^{-1} range) were utilised to account matrix effects. Polyatomic interferences were reduced by introducing a helium flux (1.0 mL min^{-1}) in the collision cell. All operating conditions used for ICP-MS assessment are listed in Table 3. The limit of detection (LOD) and the limit of quantification (LOQ) were calculated by the $3\sigma/m$ and $10\sigma/m$ criteria, respectively, where σ is the standard deviation of eleven measurements of a blank and m is the slope of the standard addition calibration. LOD and LOQ values of 0.0063 and 0.0208 μgAg g^{-1} were obtained, respectively.

2.6. AgNPs isolation from textiles

AgNPs isolation from textiles was performed by mixing 0.4000 g of textile pieces with 10 mL of ultrapure water into a plastic tube, followed by mechanical extraction at controlled temperature (20 °C) for 30 min at 100 rpm orbital-horizontal shaking. The procedure was carried out in triplicate for each sample, and two blanks were prepared for each sample set. Extracts were filtered through 5.0 μm filters for fluff removal and were conveniently diluted before spICP-MS determination (extracts were sonicated for 1.0 min before their dilution and spICP-MS analysis to avoid AgNPs agglomeration).

Furthermore, six consecutive extractions from fabric T5 were performed to evaluate the AgNPs release pattern. Conditions imply 0.4000 g of sample, 10 mL of water, mechanical shaking at 100 rpm and 20 °C for 30 min. The extracts were filtered (5.0 μm filter) and analysed by spICP-MS.

2.7. AgNPs determination/characterisation by spICP-MS

AgNPs extracts were sonicated for 5.0 min at 35 kHz before their dilution and measurement to avoid nanoparticle agglomeration. ICP-MS adjustment and the assessment of sample aspiration flow rate were performed daily. Transport efficiency (TE%) determination (particle frequency method described by Pace et al. [34]) by using AuNPs aqueous suspension (particle concentration of 518 ng L^{-1} and 60 nm nominal diameter) was also daily carried out before spICP-MS (Syngistix™ Nano Application software). Since the instrument is equipped with a cyclonic spray chamber, low TE% values (close to 5%) have been obtained. Recent reports have shown higher TE% when using linear pass spray chambers [42]. An ionic silver aqueous calibration (0–5 μg L^{-1}) was performed for the AgNPs particle size distribution assessment, whereas the NPs concentration was calculated by the frequency of NPs events [34,35]. Table 3 shows spICP-MS instrumental conditions used for AgNPs determination.

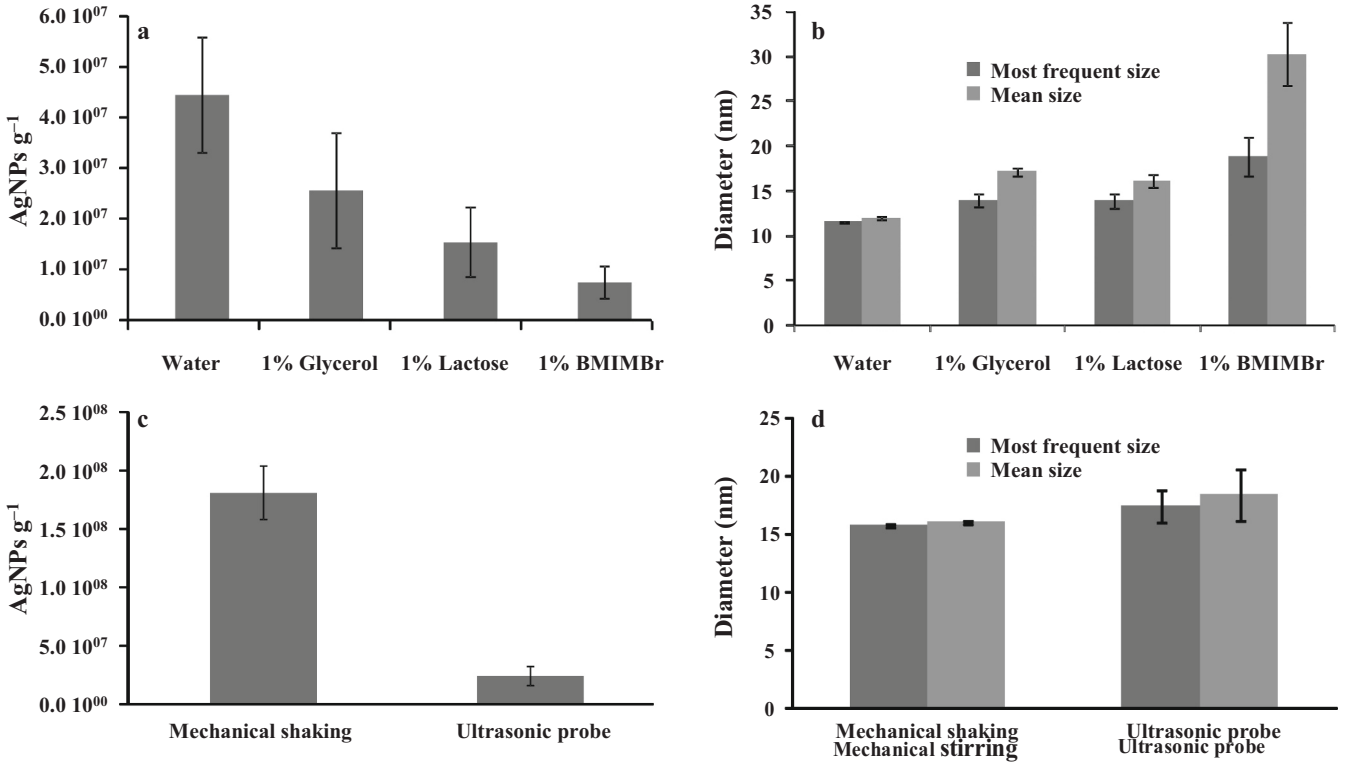

Fig. 1. Effect of the extraction solvent (continuous ultrasound extraction at 60% amplitude for 15 min) on AgNPs concentration (a) and size distribution (b); and effect of ultrasound assistance (water as a solvent, continuous ultrasound extraction at 60% amplitude for 15 min) and mechanical shaking (water as a solvent, shaking speed at 190 rpm for 12 h) on AgNPs concentration (c) and size distribution (d).

2.8. AgNPs determination/characterisation by HRTEM-EDX

An aqueous extract from fabric T6–1 (one extraction cycle, 20 °C, 30 min, and 100 rpm) was also analysed by high resolution transmission electron microscopy coupled to energy-dispersive X-ray spectroscopy (HRTEM-EDX) for comparative purposes. Due to the limit of detection of HRTEM-EDX (mg L^{-1}), a preliminary sample preconcentration step was therefore required. Preconcentration (and clean-up) of the aqueous extract was carried out using an Amicon® Ultra-0.5 centrifugal filter device. 500 μL aliquot of the aqueous extract (textile T6–1) was introduced in an Amicon device and ultracentrifuged at 14,000 g and 4 °C for 20 min, which led an extract volume of approximately 17 μL. The preconcentrated extracts were further cleaned by adding 500 μL of ultrapure water to the filter and performing a new ultracentrifugation step (14,000 g, 4 °C, and 20 min). This cleaning step with water was repeated five times. The final cleaning step was performed using the same ultracentrifugation rate and temperature, but for 10 min to allow the collection of a sample's volume of approximately 23 μL. After the cleaning steps, the filter device was placed upside down in a clean microcentrifuge tube, and centrifugation at 1000 g for 2 min was performed to transfer the concentrated and clean extract from the filter device to the collecting tube prior to analysis by HRTEM-EDX.

3. Results and discussion

3.1. Preliminary studies: Selection of the extraction solvent and the extraction technique

Studies on the release of nanoparticles from fabrics have been focused on the simulation of home laundering to assess the possible presence of nanomaterials in wastewaters and thus in the environment. Nevertheless, changes in the speciation of silver species released during textile washing procedure with detergents were proved by several authors, mainly the formation of AgNPs [28,30], and AgClNPs and Ag_2SNPs [28–30,33]. Furthermore, detergents with oxidising agents were also demonstrated to alter AgNPs size distribution and promote AgNPs dissolution [33,47]. Detergents were therefore not considered in our study due to the numerous modifications or damages they can cause to AgNPs integrity.

In addition to water [32,48–51], aqueous solutions of glycerol, lactose, and BMIMBr (1.0% *w/v*) were evaluated as potential extractants since several published articles demonstrated that ionic liquids, polyalcohols, and carbohydrates are stabilising agents of NPs and prevent agglomeration [52–54].

Ultrasonication (60% of amplitude and continuous mode for 15 min) was used for assisting the extraction (0.4000 g of textile and 10 mL of solvent) before spICP-MS assessment. Test tubes were placed into an ice bath during extraction to avoid sample's heating which could damage AgNPs. Number concentrations of AgNPs extracted are shown in Fig. 1a for experiments in triplicate and after subtracting values derived from solvent blanks analysis. Results (Fig. 1b) showed that extracted AgNPs in BMIMBr exhibited larger size distribution than those observed for the other tested solvents, which implies that BMIMBr enhanced AgNPs agglomeration. Water, glycerol, and lactose solutions led to AgNPs size distributions in which the average size and the most frequent size were quite similar. In addition, as shown in Fig. 1a, higher extraction efficiencies (higher AgNPs concentration) have been obtained when using water as an extracting solution. These findings could be due to a higher TE(%) of AgNPs dispersed in water than the TE(%) obtained when nebulising other solvents. However, high relative standard deviations (within the 16–44% range) have been found when assessing AgNPs concentrations with all extracting solutions. This may occur because of the wrapping of textile pieces around the tip of the ultrasonic probe, which hindered the extraction and even could damage the tip.

Extraction assistance by mechanical shaking was therefore tested and compared with ultrasonication assistance to improve repeatability

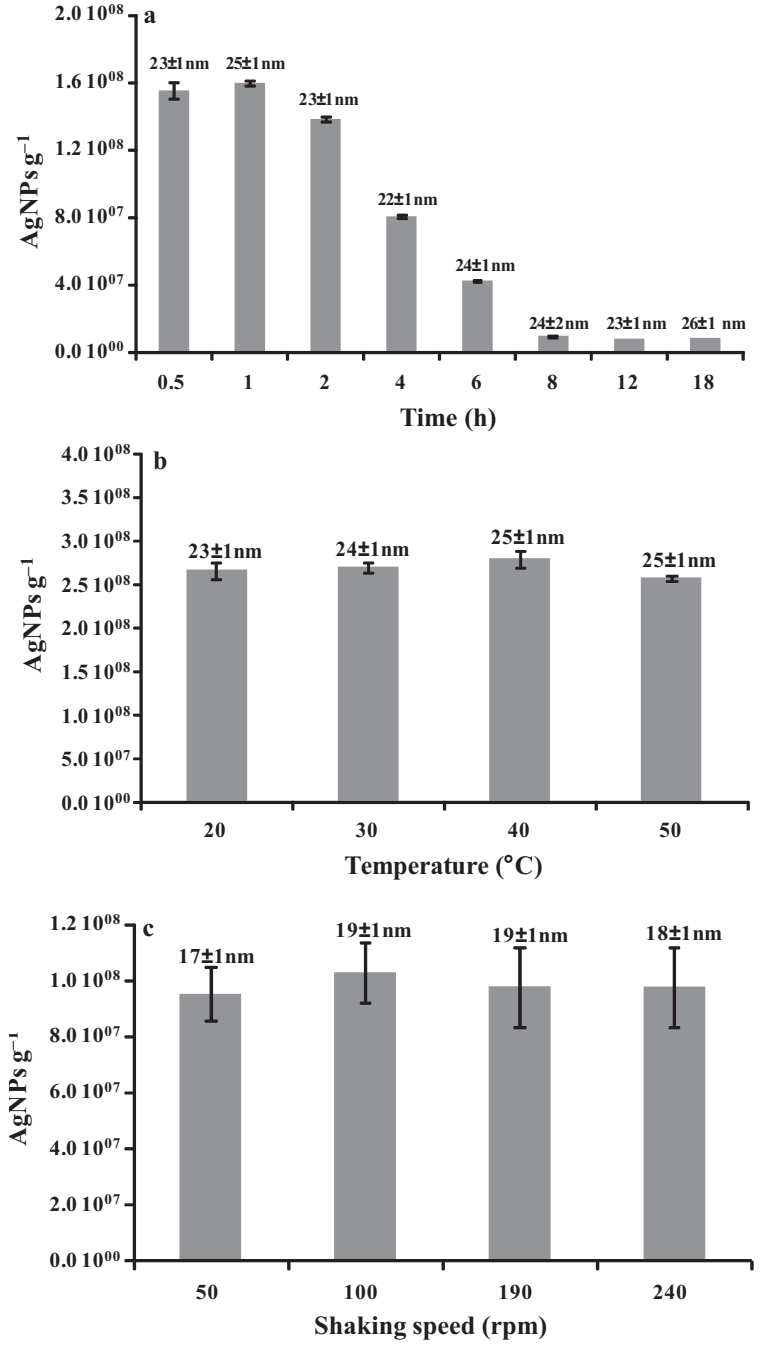

Fig. 2. Effect of mechanical shaking time (a), temperature (b), and shaking speed (c) on the AgNPs concentration [mean sizes (AgNPs size distribution) are listed onto the top of the bars].

($n = 3$). Ultrasonication conditions were the same as those used in the first experiments, and mechanical shaking consisted of orbital-horizontal shaking at 190 rpm and room temperature for 12 h (0.4000 g of textile and 10 mL of solvent). Aqueous extracts and blanks were measured in triplicate by spICP-MS. AgNPs concentration, expressed as number of AgNPs per gram, was found to be higher when applying mechanical shaking (10 times higher as shown in Fig. 1c). Fig. 1d shows that nanoparticle size distributions were similar. Mechanical shaking under controlled temperature using water as an extractant has been therefore selected for further experiments.

3.2. Mechanical shaking parameters

Parameters such as shaking time, temperature, and shaking speed were optimised. All extraction sets were performed in triplicate using 0.4000 g of a textile sample coded as T1–2. Two blanks were prepared for each extracting condition. Finally, the aqueous extracts were analysed in triplicate by spICP-MS.

3.2.1. Shaking time

Several textile subsamples were stirred using 10 mL of water at 190 rpm and room temperature for times within the range 0.5–18 h. Fig. 2a shows that similar AgNPs number concentration has been obtained for

short shaking times (0.5, 1.0, and 2.0 h), whereas the AgNPs number concentration is gradually decreased when using high shaking times. Shaking times lower than 0.5 h were not tested since similar AgNPs number concentration was observed within the 0.5–2.0 h range, and similar (or even lower) concentrations than those found for extraction times from 0.5 to 2.0 h would probably be assessed for shorter extraction times. Low AgNPs number concentration at high shaking times could be attributed to re-adsorption and/or interaction of the release AgNPs with the textile pieces and other extracted compounds. Another explanation for this behaviour could be the AgNPs dissolution at longer extraction times (a slight enhancement of ionic contents at longer times was observed, data listed in Table S1, electronic supplementary information, ESI). AgNPs size distribution has been found to be quite similar for all extracting times (mean sizes from 22 to 26 nm) as also shown in Fig. 2a. In conclusion, a shaking time of 30 min was chosen for further experiments.

3.2.2. Temperature

The effect of temperature on the AgNPs release was tested by fixing the extractant volume at 10 mL, the orbital-horizontal shaking speed at 190 rpm, and the time at 30 min. Fig. 2b shows that temperature did not affect AgNPs release from textiles, and AgNPs concentrations were quite similar (ANOVA test, 95% confidence interval) when varying the temperature within the 20–50 °C range. Similar conclusions can be attained regarding the size distribution of the extracted AgNPs, which mean sizes were quite similar under all tested temperatures. A temperature of 20 °C was therefore selected for further experiments.

3.2.3. Shaking speed

Several orbital-horizontal shaking speeds (50, 100, 190, and 240 rpm) were evaluated by applying the selected shaking temperature and time and using 10 mL of water as an extractant. Results (Fig. 2c) show a slight increase in the extracted AgNPs at high shaking speeds (100, 190, and 240 rpm). Regarding AgNPs size distributions, mean sizes when using high shaking speed were also found to be similar, which allows the selection of 100 rpm as an adequate operating value.

3.3. AgNPs stability studies during fluff removal

3.3.1. AgNPs stability during filtration (0.22 μm and 0.45 μm filters)

After extraction, some aqueous extracts could contain fluff from clothing pieces, and attempts based on filtration (mixed cellulose ester syringe filters, 0.22 μm and 0.45 μm) for fluff removal before spICP-MS were carried out. Aliquots from an aqueous extract from a textile sample (sample coded as T1–1 in Table 1), as well as AgNPs (40 and 60 nm) standards, were directly analysed by spICP-MS (unfiltered assays), and also after filtration (0.22 and 0.45 μm). Results have shown that AgNPs are partially lost during filtration of textile aqueous extracts, mainly when using 0.22 μm syringe filters ($1.67 \times 10^7 \pm 7.90 \times 10^5$ AgNPs g^{-1} in comparison to $2.00 \times 10^7 \pm 1.47 \times 10^6$ AgNPs g^{-1} after 0.45 μm filtration, and $2.26 \times 10^8 \pm 5.10 \times 10^6$AgNPs g^{-1} for unfiltered extracts). Therefore, measured AgNPs concentrations were 14 (0.22 μg filters) and 11 (0.45 μm filters) times lower after filtration. Similar results were obtained when using 40 nm AgNPs standards (AgNPs concentrations were 15 and 12 times lower after 0.22 μm and 0.45 μm filtration, respectively). AgNPs loss was found to be more important for AgNPs of larger size, and experiments carried out using 60 nm AgNPs showed that the AgNPs concentrations were 47 times (0.22 μm filtration) and 37 times (0.45 μm filtration) lower than for unfiltered 60 nm AgNPs standards. The obtained results suggest that the loss of AgNPs during filtration depends on the particle size distribution and filtration using 0.22 and 0.45 μm filters for fluff removal is not recommended.

3.3.2. AgNPs stability during centrifugation

Experiments based on centrifugation were tested to achieve the elimination of fluff in textile extracts. AgNPs suspensions (20, 40, and 60 nm) were centrifuged (3900 rpm, 4 °C, and 10 min) in triplicate. The AgNPs concentrations for centrifuged and untreated (control) solutions ($n = 9$) are shown in Fig. 3. An ANOVA test (95% confidence interval) elucidated that 20 nm AgNPs concentrations were statistically significant similar [$2.61 \times 10^{12} \pm 4.14 \times 10^{11}$ and $2.37 \times 10^{12} \pm 4.02 \times 10^{11}$ NPs L^{-1} for control and centrifuged 20 nm AgNPs standards, respectively]. Nevertheless, there were statistically significant differences between untreated and centrifuged standards when AgNPs with larger nominal diameters were used (40 and 60 nm). The loss of AgNPs during centrifugation increased with increasing AgNPs diameter (Fig. 3). Therefore, centrifugation is not advised as a methodology to remove fluff in textile extracts.

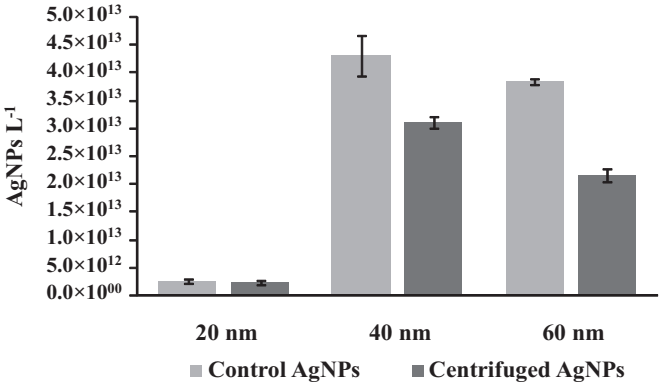

Fig. 3. Effect of centrifugation (3900 rpm, 4 °C, and 10 min) on particle concentration of AgNPs standards (Sigma-Aldrich).

Table 4
Effect of mechanical shaking (30 min, 20 °C, and 100 rpm) and filtration (syringe filters with 5.0 μm pore size) on AgNPs concentration of 20, 40, and 60 nm AgNPs standards (NanoComposix).

	AgNPs concentration (AgNPs L^{-1})		
	20 nm	40 nm	60 nm
Control	$8.75 \times 10^{13} \pm 4.01 \times 10^{12}$	$3.98 \times 10^{12} \pm 6.95 \times 10^{10}$	$4.66 \times 10^{12} \pm 4.00 \times 10^{11}$
Shaking+filtration (5.0 μm)	$8.88 \times 10^{13} \pm 2.95 \times 10^{12}$	$4.32 \times 10^{12} \pm 4.58 \times 10^{10}$	$4.92 \times 10^{12} \pm 4.43 \times 10^{11}$

3.3.3. AgNPs stability during shaking and filtration (5.0 μm filters)

Another attempt to remove fluff was the filtration of AgNPs suspensions using syringe filters with a larger pore size (5.0 μm). AgNPs suspensions (20, 40, and 60 nm) were subjected in triplicate to mechanical shaking (30 min, 20 °C, and 100 rpm) followed by 5 μm filtration, and spICP-MS assessment to test their stability under the whole proposed methodology. The same AgNPs standard solutions were also analysed without any treatment (control AgNPs), and the spICP-MS measurements were carried out in triplicate.

AgNPs concentrations ($n = 9$) for treated and untreated AgNPs (Table 4) show that shaking and filtration (5.0 μm filters) of AgNPs suspensions did not cause the loss of nanoparticles. In addition, AgNPs size distributions were not altered (the AgNPs mean sizes were 22 ± 1, 38 ± 1, and 60 ± 2 nm). Hence, AgNPs were stable using the proposed extraction methodology and filtration (5.0 μm) of AgNPs suspensions for the removal of fluff in aqueous extracts from textiles.

3.4. Validation

The limit of detection (LOD) and the limit of quantification (LOQ) of spICP-MS analysis were calculated in accordance with the $3\sigma/m$ and $10\sigma/m$ criteria, respectively, where σ is the standard deviation of the

Table 5
Silver and AgNPs concentrations in textile products.

	ICP-MS	spICP-MS [one cycle of extraction (20 °C, 30 min, and 100 rpm)]				
	Total Ag concentration ($\mu g\ g^{-1}$)[a]	AgNPs concentration (NPs g^{-1})[b]	Ionic silver concentration ($\mu g\ g^{-1}$)[b]	Nano Ag concentration ($ng\ g^{-1}$)[c]	Percentage of nano Ag released (%)[d]	Percentage of total Ag released (%)[d]
T1–2	0.489 ± 0.0236	$2.54 \times 10^6 \pm 1.92 \times 10^5$	0.034 ± 0.0005	0.245	0.05	7
T2	7.48 ± 0.235	$2.59 \times 10^7 \pm 3.35 \times 10^6$	0.25 ± 0.04	1.77	0.02	3
T3	5.83 ± 0.0668	<LOD	—[e]	—[e]	—[e]	—[e]
T4	31.2 ± 1.64	<LOD	—[e]	—[e]	—[e]	—[e]
T5	8.31 ± 0.137	$1.28 \times 10^6 \pm 1.58 \times 10^5$	0.028 ± 0.003	0.0713	0.001	0.3
T6–1	6.40 ± 0.466	$1.91 \times 10^8 \pm 2.71 \times 10^7$	0.54 ± 0.05	13.2	0.2	9
T6–2	6.02 ± 0.929	$1.22 \times 10^7 \pm 1.97 \times 10^6$	0.36 ± 0.05	4.31	0.1	6
T7	1.20 ± 0.171	$2.68 \times 10^5 \pm 4.40 \times 10^4$	0.029 ± 0.002	0.0210	0.002	2

[a] Microwave-assisted acid digestion and ICP-MS.
[b] Water extraction and spICP-MS.
[c] Theoretical Ag concentration of AgNPs considering AgNPs concentration and size distribution (water extraction and spICP-MS), assuming a spherical shape of AgNPs.
[d] Percentages (%) were referred to total Ag concentration assessed by microwave-assisted acid digestion and ICP-MS.
[e] Not assessed.

measurements of eleven blanks (10 mL of ultrapure water subjected to the optimised extraction procedure) by spICP-MS, and m is the mean slope of the ionic Ag calibration (calibration within the 0–5 $\mu g\ L^{-1}$ range). Experimental LODs and LOQs were 4.59×10^4 AgNPs g^{-1} and 1.53×10^5 AgNPs g^{-1}, respectively, after considering the sample pre-treatment used.

Furthermore, the LOD in size was calculated by applying the 3σ (or 5σ) criterion outlined by Lee et al. [55]. The calculated values were 9.8 and 11.6 nm for 3σ and 5σ criteria, respectively.

The precision of the developed procedure (sample pre-treatment and spICP-MS assessment) was expressed through the relative standard deviation (RSD) after subjecting a textile sample (sample coded as T6–1) to the proposed procedure eleven times. The eleven extracts were further analysed by spICP-MS in triplicate, and the found AgNPs concentration (mean ± standard deviation) was $1.91 \times 10^8 \pm 2.71 \times 10^7$ AgNPs g^{-1}, which implies a RSD value of 14%. Regarding AgNPs size distribution, mean size of 23 ± 1 nm (RSD value of 6%) was obtained. Consequently, the methodology has been therefore to be precise.

The accuracy of spICP-MS measurements was tested by analytical recovery assays. Three aliquots from the same extract from a textile sample containing AgNPs were spiked with AgNPs standards of several nominal diameters (20, 40, or 60 nm). The spiked extracts as well as unspiked extracts (three replicates), and the AgNPs suspensions used for spiking (suspensions at the same AgNPs concentration as those used for spiking experiments) were measured by spICP-MS in triplicate. Therefore, the assay implied nine measurements of each solution (unspiked extracts, extracts spiked with AgNPs of different nominal sizes, and AgNPs solutions of different nominal sizes). Analytical recoveries were calculated as the ratio (×100) of the difference between the AgNPs concentrations of spiked and unspiked extracts, and the concentrations of AgNPs standards used for spiking. Results have shown good accuracy for the spICP-MS measurements because analytical recoveries were close to 100% for all AgNPs sizes (113 ± 5%, 102 ± 6%, and 106 ± 2% for 20, 40, and 60 nm AgNPs standards, respectively)..

3.5. Application

The proposed method was applied to seven textiles, three of them (samples coded as T5, T6, and T7) were commercialised as textiles containing nanosilver, and the remaining textiles (T1, T2, T3, and T4) as products containing silver. Subsamples (T1–2, and T6–1 and T6–2) were considered from textiles T1 (cycling sportswear) and T6 (socks) because

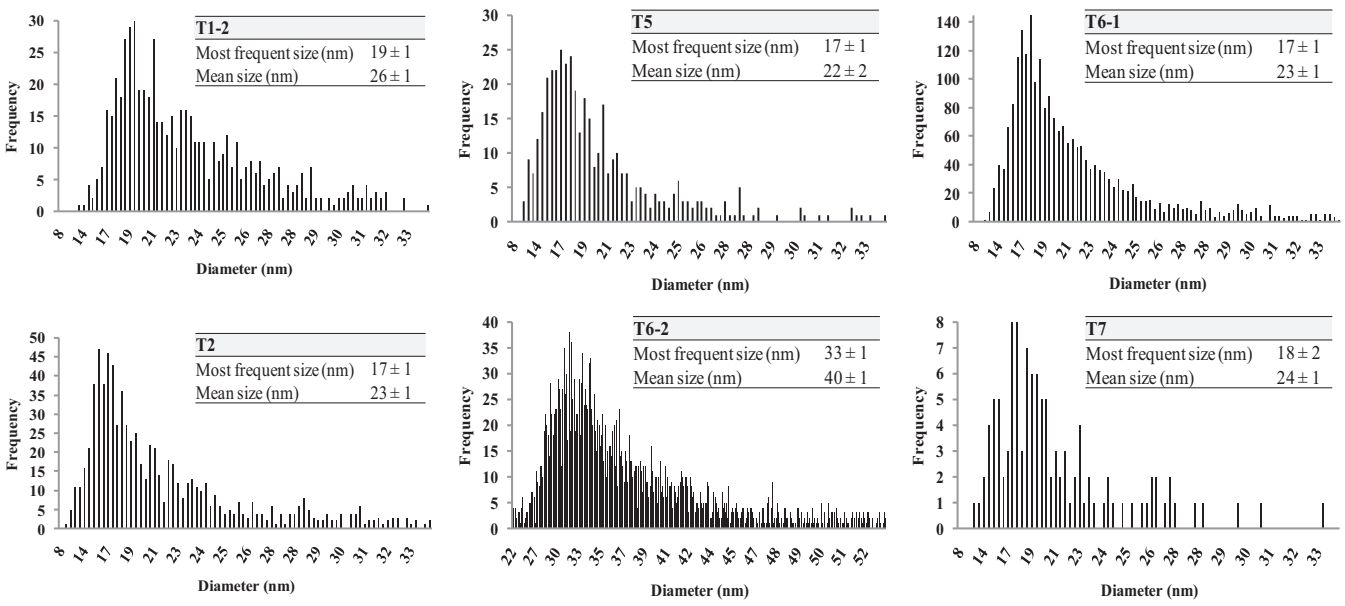

Fig. 4. Size distribution of AgNPs in textiles containing silver (T1–2 and T2) and textiles containing nanosilver (T5, T6–1, T6–2, and T7) obtained by spICP-MS.

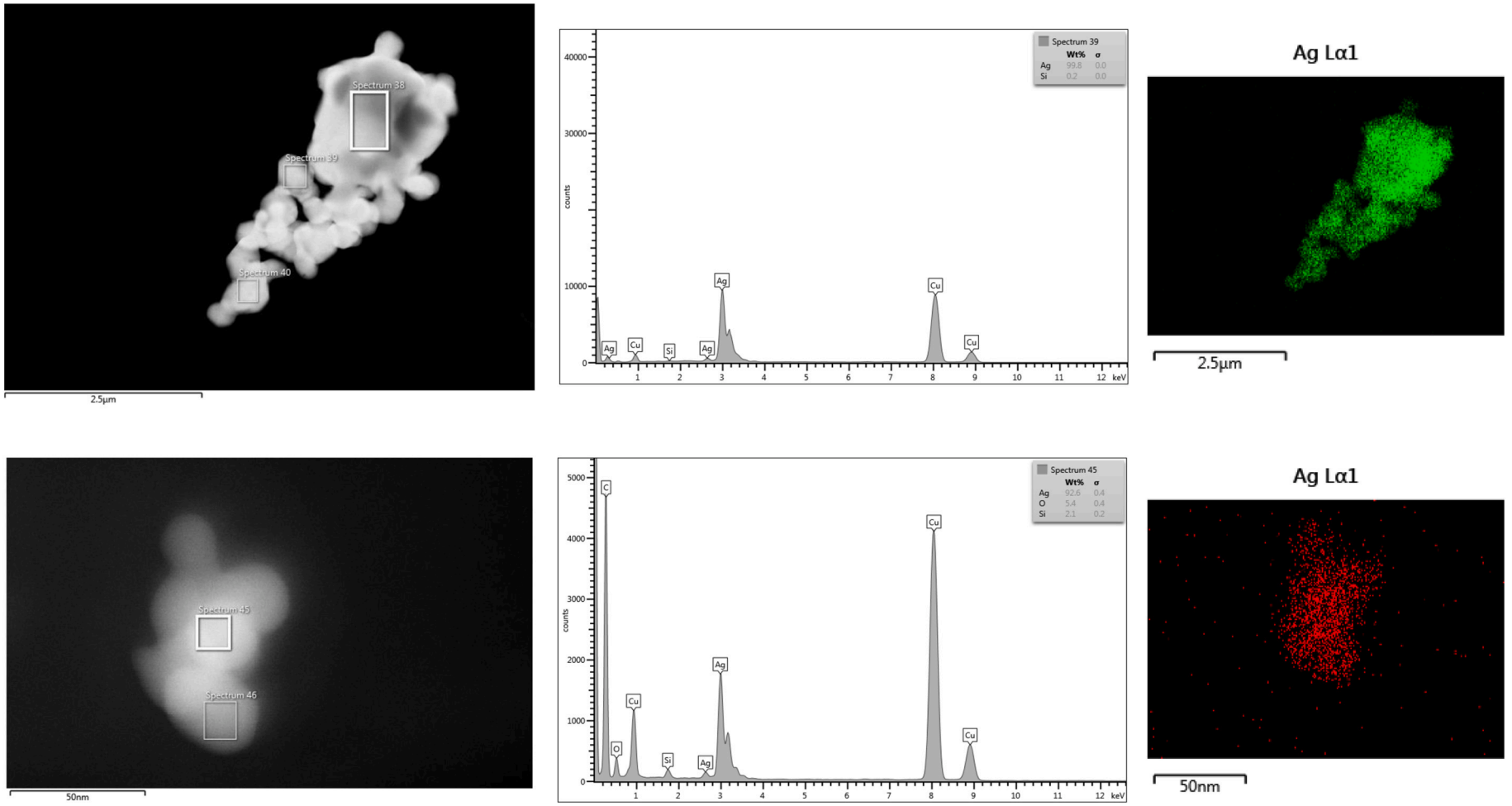

Fig. 5. HRTEM-EDX analysis of a concentrated and clean aqueous extract from fabric T6–1 after one cycle of extraction.

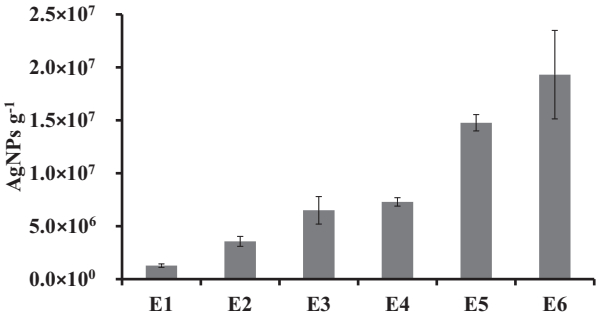

Fig. 6. Particle number concentrations of AgNPs in aqueous leachates from fabric T5 after subjecting six consecutive extraction cycles using the optimised extraction conditions (the letter "E" followed by a number denotes the extraction number).

of the different appearance of fibres. All samples were analysed for total silver (microwave-assisted acid digestion and ICP-MS measurement) and for AgNPs determinations (proposed extraction procedure followed by spICP-MS). Table 5 lists the total silver concentrations determined in textile samples (microwave-assisted acid digestion and ICP-MS measurement) as well as AgNPs concentrations and ionic silver concentrations in aqueous extracts (proposed extraction procedure and spICP-MS analysis); whereas data regarding AgNPs size distribution are given in Figs. 4 (a-b). Table 5 also shows the silver concentration (and the silver percentage) derived from the assessed AgNPs considering the mean AgNPs concentrations and the mean AgNPs sizes obtained. Assumptions such as the spherical shape and solid nature of all AgNPs have been considered for these theoretical calculations.

Total Ag concentrations varied from 1.3 ± 0.1 (T7) to 10 ± 0.4 (T5) for textiles commercialised as containing nanosilver, whereas total Ag contents varied from 1.7 ± 0.3 (T1–2) to 36 ± 4 (T4) for textiles reported as containing silver.

In general, AgNPs concentrations in nanosilver textiles are slightly higher than those found in textiles commercialised as containing silver, although the latter has also shown the presence of AgNPs. Regarding size distribution [Figs. 4 (a-b)], mean sizes varied from 22 ± 2 nm (T5) to 40 ± 1 nm (T6–2), and were quite close to the most frequent size, which suggests AgNPs size distribution is nearly a normal distribution.

Silver concentrations in textiles derived from the assessed AgNPs (AgNPs concentration and size distribution, considering a spherical shape and solid nature of all AgNPs) were found to be within the 0.0210–13.2 ng g^{-1} (ng_{silver} g^{-1}_{fabric}) range [Table 5]. Percentages of nanosilver released in aqueous extracts (percentage of silver derived from extracted AgNPs referred to the total Ag concentration assessed by microwave-assisted acid digestion and ICP-MS) were therefore very low, ranging from 0.001% (T5) to 0.2% (T6–1).

Total released silver was also calculated by summing ionic silver concentrations and nanosilver concentrations (in mass units) obtained by spICP-MS analysis. Percentage of total released silver varied between 0.3% (fabric T5) and 9% (fabric T6–1) [Table 5]. Similar results were obtained by Benn et al. [49], who reported that two studied socks released less than 1% of their total silver into water after four washing cycles (agitation at 50 rpm for 24 h). In addition, Nam et al. [51] proved that 90% of total silver remained in cotton fabrics functionalised with AgNPs after ten laundering cycles (laboratory washing machine, 40 °C, 40 rpm, and 45 min).

Furthermore, AgNPs presence in an aqueous extract (fabric T6–1) was confirmed by HRTEM images and energy-dispersive X-ray analysis. AgNPs have been found to be spherical in shape and highly agglomerated (Fig. 5). The high degree of agglomeration makes difficult particle size distribution (PSD) calculations but Fig. 5 shows that the isolated AgNPs exhibit a size of approximately 20 nm, quite similar than that obtained by spICP-MS (23 ± 1 nm, Fig. 4).

Finally, due to the low percentages of silver released in the aqueous extracts from studied fabrics, consecutive extractions were performed using the developed methodology for AgNPs extraction from fabric T5, which released the lowest percentages of nanosilver (0.001%) and total silver (0.3%). Six extraction cycles using the optimal extraction conditions (10 mL of water, 30 min, 20 °C, and 100 rpm) were performed, and each consecutive extraction was carried out in triplicate, and two blanks were performed for each condition. Fig. 6 shows a progressive enhancement of extracted AgNPs from fabric T5 with increasing extraction cycle number. This release pattern can be attributed to the fact that AgNPs were strongly integrated into the fibres and their release occurred slowly over several extraction cycles. In this way, Mitrano et al. [28] previously demonstrated that the release rate of AgNPs is lower in fabrics in which NPs are embedded in the fibres than in fabrics modified with NPs on the surface.

4. Conclusions

Silver nanoparticles releasing from (nano)textiles has been found to be a difficult task since the high degree of fixation of the nanoparticles to the fabrics, which would require the use of strong extractive conditions for an exhaustive extraction. However, AgNPs are highly ionizable and soft extractive conditions are needed for guaranteeing the integrity of the released nanoparticles. Therefore, the proposed extraction procedure (orbital-horizontal shaking using ultrapure water as an extractant) has led to non-quantitative AgNPs extractions but interesting findings about the characterization (size distribution) of isolated AgNPs have been found when using spICP-MS for detection. Despite the extraction was non-quantitative, spICP-MS methodology has been demonstrated to be highly sensitive (AgNPs number concentration and AgNPs size) as well as precise and accurate. Percentages of nanosilver released from studied fabrics varied from 0.001 to 0.2%, and AgNPs mean sizes were found to be within the 22–40 nm range. HRTEM-EDX analysis also confirmed the presence of AgNPs in the extracts.

CRediT authorship contribution statement

Iria Rujido-Santos: Formal analysis, Investigation, Validation, Visualization, Writing – original draft. **M. Estela del Castillo Busto:** Investigation, Validation, Writing – review & editing. **Isabel Abad-Alvaro:** Investigation, Validation, Writing – review & editing. **Paloma Herbello-Hermelo:** Data curation, Supervision, Software, Validation. **Pilar Bermejo-Barrera:** Resources, Project administration, Funding acquisition, Writing – review & editing. **María Carmen Barciela-Alonso:** Data curation, Supervision, Writing – review & editing. **Heidi Goneaga-Infante:** Supervision, Resources, Writing – review & editing. **Antonio Moreda-Piñeiro:** Conceptualization, Methodology, Validation, Writing – review & editing, Supervision.

Declaration of Competing Interest

None.

Data availability

Data will be made available on request.

Acknowledgments

The authors wish to acknowledge the financial support of the Ministerio de Economía y Competitividad (projects INNOVANANO, reference RT2018–099222-B-100), and the Xunta de Galicia (Grupo de Referencia Competitiva, grant number ED431C2018/19). I. Rujido-Santos thanks the Xunta de Galicia and the European Social Fund (FSE) for a pre-doctoral grant (ref. ED481A-2018/127). The authors also thank Dra. Mª José Pazos Guldrís (*Unidade de Microscopía Electrónica e*

Confocal e de Apoio ás Especialidades Biolóxicas at the University of Santiago de Compostela) for HRTEM-EDX technical support.

Appendix A. Supplementary data

Supplementary data to this article can be found online at https://doi.org/10.1016/j.sab.2022.106505.

References

[1] M. Rai, A. Yadav, A. Gade, Silver nanoparticles as a new generation of antimicrobials, Biotechnol. Adv. 27 (2009) 76–83, https://doi.org/10.1016/j.biotechadv.2008.09.002.

[2] K. Wang, J. He, One-pot fabrication of antireflective/antibacterial dual-function Ag NP-containing mesoporous silica thin films, ACS Appl. Mater. Interfaces 10 (2018) 11189–11196, https://doi.org/10.1021/acsami.8b00192.

[3] P. Balashanmugam, M.D. Balakumaran, R. Murugan, K. Dhanapal, P. T. Kalaichelvan, Phytogenic synthesis of silver nanoparticles, optimization and evaluation of *in vitro* antifungal activity against human and plant pathogens, Microbiol. Res. 192 (2016) 52–64, https://doi.org/10.1016/j.micres.2016.06.004.

[4] T.Q. Huy, N.T.H. Thanh, N.T. Thuy, P.V. Chung, P.N. Hung, A.T. Le, N.T.H. Hanh, Cytotoxicity and antiviral activity of electrochemical-synthesized silver nanoparticles against poliovirus, J. Virol. Methods 241 (2017) 52–57, https://doi.org/10.1016/j.jviromet.2016.12.015.

[5] K. Chaloupka, Y. Malam, A.M. Seifalian, Nanosilver as a new generation of nanoproduct in biomedical applications, Trends Biotechnol. 28 (2010) 580–588, https://doi.org/10.1016/j.tibtech.2010.07.006.

[6] K. Venugopal, H.A. Rather, K. Rajagopal, M.P. Shanthi, K. Sheriff, M. Illiyas, R. A. Rather, E. Manikandan, S. Uvarajan, M. Bhaskar, M. Maaza, Synthesis of silver nanoparticles (Ag NPs) for anticancer activities (MCF 7 breast and A549 lung cell lines) of the crude extract of *Syzygium aromaticum*, J. Photochem. Photobiol. B 167 (2017) 282–289, https://doi.org/10.1016/j.jphotobiol.2016.12.013.

[7] K.A. Homan, M. Souza, R. Truby, G.P. Luke, C. Green, E. Vreeland, S. Emelianov, Silver nanoplate contrast agents for in vivo molecular photoacoustic imaging, ACS Nano 6 (2012) 641–650, https://doi.org/10.1021/nn204100n.

[8] S.M. Praveena, K. Karuppiah, L.T.L. Than, Potential of cellulose paper coated with silver nanoparticles: a benign option for emergency drinking water filter, Cellulose 25 (2018) 2647–2658, https://doi.org/10.1007/s10570-018-1747-x.

[9] K. Ramos, M.M. Gómez-Gómez, C. Cámara, L. Ramos, Silver speciation and characterization of nanoparticles released from plastic food containers by single particle ICPMS, Talanta 151 (2016) 83–90, https://doi.org/10.1016/j.talanta.2015.12.071.

[10] S. Kokura, O. Handa, T. Takagi, T. Ishikawa, Y. Naito, T. Yoshikawa, Silver nanoparticles as a safe preservative for use in cosmetics, Nanomed. Nanotechnol. Biol. Med. 6 (2010) 570–574, https://doi.org/10.1016/j.nano.2009.12.002.

[11] J. Farkas, H. Peter, P. Christian, J.A. Gallego Urrea, M. Hassellöv, J. Tuoriniemi, S. Gustafsson, E. Olsson, K. Hylland, K.V. Thomas, Characterization of the effluent from a nanosilver producing washing machine, Environ. Int. 37 (2011) 1057–1062, https://doi.org/10.1016/j.envint.2011.03.006.

[12] R. Kaegi, B. Sinnet, S. Zuleeg, H. Hagendorfer, E. Mueller, R. Vonbank, M. Boller, M. Burkhardt, Release of silver nanoparticles from outdoor facades, Environ. Pollut. 158 (2010) 2900–2905, https://doi.org/10.1016/j.envpol.2010.06.009.

[13] M. Radetić, Functionalization of textile materials with silver nanoparticles, J. Mater. Sci. 48 (2013) 95–107, https://doi.org/10.1007/s10853-012-6677-7.

[14] W. Feng, T. Huang, L. Gao, X. Yang, W. Deng, R. Zhou, H. Liu, Textile-supported silver nanoparticles as a highly efficient and recyclable heterogeneous catalyst for nitroaromatic reduction at room temperature, RSC Adv. 8 (2018) 6288–6292, https://doi.org/10.1039/C7RA13257C.

[15] D.Q. Vo, E.W. Shin, J.S. Kim, S. Kim, Low-temperature preparation of highly conductive thin films from acrylic acid-stabilized silver nanoparticles prepared through ligand exchange, Langmuir 26 (2010) 17435–17443, https://doi.org/10.1021/la102627m.

[16] G. Montes-Hernandez, M. Di Girolamo, G. Sarret, S. Bureau, A. Fernandez-Martinez, C. Lelong, E., Eymard vernain, in situ formation of silver nanoparticles (Ag-NPs) onto textile fibers, ACS Omega 6 (2021) 1316–1327, https://doi.org/10.1021/acsomega.0c04814.

[17] Q. Xu, R. Li, L. Shen, W. Xu, J. Wang, Q. Jiang, L. Zhang, F. Fu, Y. Fu, X. Liu, Enhancing the surface affinity with silver nano-particles for antibacterial cotton fabric by coating carboxymethyl chitosan and L-cysteine, Appl. Surface Sci. 497 (2019), 143673, https://doi.org/10.1016/j.apsusc.2019.143673.

[18] R. Dastjerdi, M. Montazer, A review on the application of inorganic nano-structured materials in the modification of textiles: Focus on anti-microbial properties, Colloids Surf. B 79 (2010) 5–18, https://doi.org/10.1016/j.colsurfb.2010.03.029.

[19] Y.Y. Zhang, Q.B. Xu, F.Y. Fu, X.D. Liu, Durable antimicrobial cotton textiles modified with inorganic nanoparticles, Cellulose 23 (2016) 2791–2808, https://doi.org/10.1007/s10570-016-1012-0.

[20] F.M. Kelly, J.H. Johnston, Colored and functional silver nanoparticle−wool fiber composites, ACS Appl. Mater. Interfaces 3 (2011) 1083–1092, https://doi.org/10.1021/am101224v.

[21] B. Tang, M. Zhang, X. Hou, J. Li, L. Sun, X. Wang, Coloration of cotton fibers with anisotropic silver nanoparticles, Ind. Eng. Chem. Res. 51 (2012) 12807–12813, https://doi.org/10.1021/ie3015704.

[22] B. Tang, J. Li, X. Hou, T. Afrin, L. Sun, X. Wang, Colorful and antibacterial silk fiber from anisotropic silver nanoparticles, Ind. Eng. Chem. Res. 52 (2013) 4556–4563, https://doi.org/10.1021/ie3033872.

[23] H.E. Emam, S. Mowafi, H.M. Mashaly, M. Rehan, Production of antibacterial colored viscose fibers using in situ prepared spherical Ag nanoparticles, Carbohydr. Polym. 110 (2014) 148–155, https://doi.org/10.1016/j.carbpol.2014.03.082.

[24] B.J. Brüschweiler, C. Merlot, Azo dyes in clothing textiles can be cleaved into a series of mutagenic aromatic amines which are not regulated yet, Regul. Toxicol. Pharmacol. 88 (2017) 214–226, https://doi.org/10.1016/j.yrtph.2017.06.012.

[25] S. Perera, B. Bhushan, R. Bandara, G. Rajapakse, S. Rajapakse, C. Bandara, Morphological, antimicrobial, durability, and physical properties of untreated and treated textiles using silver-nanoparticles, Colloids Surf. A Physicochem. Eng. Asp. 436 (2013) 975–989, https://doi.org/10.1016/j.colsurfa.2013.08.038.

[26] M.E.K. Kraeling, V.D. Topping, Z.M. Keltner, K.R. Belgrave, K.D. Bailey, X. Gao, J. J. Yourick, *In vitro* percutaneous penetration of silver nanoparticles in pig and human skin, Regul. Toxicol. Pharmacol. 95 (2018) 314–322, https://doi.org/10.1016/j.yrtph.2018.04.006.

[27] F.F. Larese, F. D'Agostin, M. Crosera, G. Adami, N. Renzi, M. Bovenzi, G. Maina, Human skin penetration of silver nanoparticles through intact and damaged skin, Toxicology 255 (2009) 33–37, https://doi.org/10.1016/j.tox.2008.09.025.

[28] D.M. Mitrano, E. Rimmele, A. Wichser, R. Erni, M. Height, B. Nowack, Presence of nanoparticles in wash water from conventional silver and nano-silver textiles, ACS Nano 8 (2014) 7208–7219, https://doi.org/10.1021/nn502228w.

[29] C. Lorenz, L. Windler, N. von Goetz, R.P. Lehmann, M. Schuppler, K. Hungerbühler, M. Heuberger, B. Nowack, Characterization of silver release from commercially available functional (nano)textiles, Chemosphere 89 (2012) 817–824, https://doi.org/10.1016/j.chemosphere.2012.04.063.

[30] E. Lombi, E. Donner, K.G. Scheckel, R. Sekine, C. Lorenz, N. Von Goetz, B. Nowack, Silver speciation and release in commercial antimicrobial textiles as influenced by washing, Chemosphere 111 (2014) 352–358, https://doi.org/10.1016/j.chemosphere.2014.03.116.

[31] L. Geranio, M. Heuberger, B. Nowack, The behavior of silver nanotextiles during washing, Environ. Sci. Technol. 43 (2009) 8113–8118, https://doi.org/10.1021/es9018332.

[32] R.B. Reed, T. Zaikova, A. Barber, M. Simonich, R. Lankone, M. Marco, K. Hristovski, P. Herckes, L. Passantino, D.H. Fairbrother, R. Tanguay, J. F. Ranville, J.E. Hutchison, P.K. Westerhoff, Potential environmental impacts and antimicrobial efficacy of silver- and nanosilver-containing textiles, Environ. Sci. Technol. 50 (2016) 4018–4026, https://doi.org/10.1021/acs.est.5b06043.

[33] D.M. Mitrano, E. Lombi, Y.A.R. Dasilva, B. Nowack, Unraveling the complexity in the aging of nanoenhanced textiles: a comprehensive sequential study on the effects of sunlight and washing on silver nanoparticles, Environ. Sci. Technol. 50 (2016) 5790–5799, https://doi.org/10.1021/acs.est.6b01478.

[34] H.E. Pace, N.J. Rogers, C. Jarolimek, V.A. Coleman, C.P. Higgins, J.F. Ranville, Determining transport efficiency for the purpose of counting and sizing nanoparticles via single particle inductively coupled plasma mass spectrometry, Anal. Chem. 83 (2011) 9361–9369, https://doi.org/10.1021/ac201952t.

[35] F. Laborda, E. Bolea, J. Jiménez-Lamana, Single particle inductively coupled plasma mass spectrometry: a powerful tool for nanoanalysis, Anal. Chem. 86 (2014) 2270–2278, https://doi.org/10.1021/ac402980q.

[36] F. Laborda, E. Bolea, J. Jiménez-Lamana, Single particle inductively coupled plasma mass spectrometry for the analysis of inorganic engineered nanoparticles in environmental samples, Trends Environ. Anal. Chem. 9 (2016) 15–23, https://doi.org/10.1016/j.teac.2016.02.001.

[37] M.D. Montaño, J.W. Olesik, A.G. Barber, K. Challis, J.F. Ranville, Single Particle ICP-MS: Advances toward routine analysis of nanomaterials, Anal. Bioanal. Chem. 408 (2016) 5053–5074, https://doi.org/10.1007/s00216-016-9676-8.

[38] D. Mozhayeva, C. Engelhard, A critical review of single particle inductively coupled plasma mass spectrometry-A step towards an ideal method for nanomaterial characterization, J. Anal. At. Spectrom. 35 (2020) 1740–1783, https://doi.org/10.1039/c9ja00206e.

[39] B.M. Freire, Y.T. Cavalcanti, C.N. Lange, J.C. Pieretti, R.M. Pereira, M. C. Gonçalves, G. Nakazato, A.B. Seabra, B.L. Batista, Evaluation of collision/reaction gases in single-particle ICP-MS for sizing selenium nanoparticles and assessment of their antibacterial activity, Nanotechnology 33 (2022), 355702, https://doi.org/10.1088/1361-6528/ac723e.

[40] C. Suárez-Oubiña, P. Herbello-Hermelo, P. Bermejo-Barrera, A. Moreda-Piñeiro, Single-particle inductively coupled plasma mass spectrometry using ammonia reaction gas as a reliable and free-interference determination of metallic nanoparticles, Talanta 242 (2022), 123286, https://doi.org/10.1016/j.talanta.2022.123286.

[41] O. Geiss, I. Bianchi, G. Bucher, E. Verleysen, F. Brassinne, J. Mast, K. Loeschner, L. Givelet, F. Cubadda, F. Ferraris, A. Raggi, F. Iacoponi, R. Peters, A. Undas, A. Müller, A.-K. Meinhardt, B. Hetzer, V. Gräf, A.R. Montoro Bustos, J. Barrero-Moreno, Determination of the transport efficiency in spICP-MS analysis using conventional sample introduction systems: an interlaboratory comparison study, Nanomaterials 12 (2022) 725, https://doi.org/10.3390/nano12040725.

[42] D. Ojeda, E. Bolea, J. Pérez-Arantegui, F. Laborda, Exploring the boundaries in the analysis of large particles by single particle inductively coupled plasma mass spectrometry: Application to nanoclays, J. Anal. At. Spectrom. 37 (2022) 1501, https://doi.org/10.1039/d2ja00026a.

[43] M. Aramendía, J.C. García-Mesa, E.V. Alonso, R. Garde, A. Bazo, J. Resano, M. Resano, A novel approach for adapting the standard addition method to single particle-ICP-MS for the accurate determination of NP size and number concentration in complex matrices, Anal. Chim. Acta 1205 (2022), 339738, https://doi.org/10.1016/j.aca.2022.339738.

[44] S. Harycki, A. Gundlach-Graham, Online microdroplet calibration for accurate nanoparticle quantification in organic matrices, Anal. Bioanal. Chem. (2022), https://doi.org/10.1007/s00216-022-04115-2 in press.
[45] M. Bierwirth, V. Olszok, A. Wollmann, A.P. Weber, A new coupling setup of DMA, CPC and sp-ICP-MS with increased versatility, J. Aerosol Sci. 163 (2022), 105983, https://doi.org/10.1016/j.jaerosci.2022.105983.
[46] M.E. Johnson, J. Bennett, A.R. Montoro Bustos, S.K. Hanna, A. Kolmakov, N. Sharp, E.J. Petersen, P.E. Lapasset, C.M. Sims, K.E. Murphy, B.C. Nelson, Combining secondary ion mass spectrometry image depth profiling and single particle inductively coupled plasma mass spectrometry to investigate the uptake and biodistribution of gold nanoparticles in Caenorhabditis elegans, Anal. Chim. Acta 1175 (2021) 338671, https://doi.org/10.1016/j.aca.2021.338671.
[47] D.M. Mitrano, Y.A.R. Dasilva, B. Nowack, Effect of variations of washing solution chemistry on nanomaterial physicochemical changes in the laundry cycle, Environ. Sci. Technol. 49 (2015) 9665–9673, https://doi.org/10.1021/acs.est.5b02262.
[48] E. Spielman-Sun, T. Zaikova, T. Dankovich, J. Yun, M. Ryan, J.E. Hutchison, G. V. Lowry, Effect of silver concentration and chemical transformations on release and antibacterial efficacy in silver-containing textiles, NanoImpact 11 (2018) 51–57, https://doi.org/10.1016/j.impact.2018.02.002.
[49] T.M. Benn, P. Westerhoff, Nanoparticle silver released into water from commercially available sock fabrics, Environ. Sci. Technol. 42 (2008) 4133–4139, https://doi.org/10.1021/es7032718.
[50] A. Mackevica, M.E. Olsson, S.F. Hansen, Quantitative characterization of TiO_2 nanoparticle release from textiles by conventional and single particle ICP-MS, J. Nanopart. Res. 20 (2018) 6, https://doi.org/10.1007/s11051-017-4113-2.
[51] S. Nam, M.B. Hillyer, B.D. Condon, J.S. Lum, M.N. Richards, Q. Zhang, Silver nanoparticle-infused cotton fiber: durability and aqueous release of silver in laundry water, J. Agric. Food Chem. 68 (2020) 13231–13240, https://doi.org/10.1021/acs.jafc.9b07531.
[52] J. Łuczak, M. Paszkiewicz, A. Krukowska, A. Malankowska, A. Zaleska-Medynska, Ionic liquids for nano- and microstructures preparation. Part 1: Properties and multifunctional role, Adv. Colloid Interf. Sci. 230 (2016) 13–28, https://doi.org/10.1016/j.cis.2015.08.006.
[53] G. Clergeaud, R. Genç, M. Ortiz, C.K. O'Sullivan, Liposomal nanoreactors for the synthesis of monodisperse palladium nanoparticles using glycerol, Langmuir 29 (2013) 15405–15413, https://doi.org/10.1021/la402892f.
[54] A. Sobhani-Nasab, M. Behpour, Synthesis, characterization, and morphological control of $Eu_2Ti_2O_7$ nanoparticles through green method and its photocatalyst application, J. Mater. Sci. Mater. Electron. 27 (2016) 11946–11951, https://doi.org/10.1007/s10854-016-5341-4.
[55] S. Lee, X. Bi, R.B. Reed, J.F. Ranville, P. Herckes, P. Westerhoff, Nanoparticle size detection limits by single particle ICP-MS for 40 elements, Environ. Sci. Technol. 48 (2014) 10291–10300, https://doi.org/10.1021/es502422v.